ELSEVIER

International Journal of Mass Spectrometry 221 (2002) 191–207

International Journal of Mass Spectrometry

www.elsevier.com/locate/ijms

Probing mass discriminations and mass shifts in the ITMS mass spectra of externally generated MALDI ions with synthetic polymers

G.J. van Rooij, J.J. Boon, M.C. Duursma, R.M.A. Heeren*

Unit for Macromolecular Mass Spectrometry, FOM-Institute for Atomic and Molecular Physics, Kruislaan 407, 1098 SJ Amsterdam, The Netherlands

Received 18 July 2002; accepted 11 September 2002

Abstract

Synthetic polymers are demonstrated to be very useful probes for the characterization of a newly constructed external ion source matrix-assisted laser desorption and ionization quadrupole ion trap mass spectrometer (MALDI-ITMS). Mass discrimination effects and space-charge-induced mass shifts can readily be identified and quantified with these synthetic polymer probes. Mass dependencies in the trapping efficiency were evaluated by comparison of measurements of poly(methyl methacrylate) (PMMA) standards in the mass range *m/z* 400–3400 with MALDI-TOF-MS measurements of the same samples. This established the optimal experimental conditions for the analysis of mass ranges smaller than 1000 u with negligible mass discrimination. This is demonstrated on the basis of measurements on a tri-block copolymer of poly(ethylene oxide) poly(propylene oxide). As expected, mass measurements were highly influenced by the magnitude of the trapped ion population. Using poly(ethylene glycol) standards we were able to quantify these mass shifts as a function of the total ion load. Consequently, reproducible results can only be obtained by reproducing the total space-charge in the trap. In MALDI experiments, this can be achieved by tuning the laser power just above threshold. This approach allowed the mass determination of three different end groups in a complex Jeffamine D2000 sample with an accuracy of better than 0.1 u. (Int J Mass Spectrom 221 (2002) 191–207)

Keywords: MALDI-ITMS; Synthetic polymers; Molecular weight distribution; Space-charge

1. Introduction

For mass spectrometric characterization of large molecules, soft ionization techniques which minimize fragmentation during ionization and thus produce (pseudo) molecular ions, have proven to be most successful for lifting and converting the molecules from the condensed phase to gaseous ions. Within this range of techniques, especially electrospray ionization [1] and matrix-assisted laser desorption/ionization (MALDI) [2] have proven their importance in providing accurate and detailed molecular weight data on high molecular weight materials. Additional properties of MALDI that make it especially suited for many applications include the dominance of singly-charged (pseudo) molecular ions (which makes the resulting mass spectra easy to interpret) and its tolerance for salts, buffers and other common additives and impurities. Since its introduction by Karas and Hillenkamp [3] the technique has successfully been

* Corresponding author. E-mail: heeren@amolf.nl

1387-3806/02/$ – see front matter
PII S1387-3806(02)00989-2

applied to volatilize and ionize a wide variety of molecules, such as peptides, proteins, oligosaccharides, and synthetic polymers. Several reviews illustrate the continuously growing scope of MALDI applications [4–6].

Traditionally, MALDI is coupled to time-of-flight (providing high sensitivity and a theoretically unlimited mass range) [7,8] or Fourier transform ion cyclotron resonance mass spectrometers (providing superior mass accuracy and mass resolution and multistage tandem mass spectrometry) [9]. A relatively new area is the use of the quadrupole ion trap mass spectrometer (ITMS) in analytical applications of MALDI. Nevertheless, the ITMS seems particularly well-suited to these applications. For example, the pulsed nature of the ion production in a MALDI ion source matches well with the pulsed operation of the ITMS, whereas the capacity of the ITMS to store all ions created in the MALDI process, irrespective of the time scale on which these were formed, offers the possibility of panoramic registration of the ions from each laser shot. Moreover, the ITMS provides high sensitivity in the measurements and possibilities for multistage tandem mass spectrometry (MS^n). These are great potentials for the analysis of large molecules in complex mixtures.

Various publications have dealt with the coupling of MALDI and the ITMS, which was realized either by performing the MALDI ionization event near the trap or by producing MALDI ions in an external ion source and subsequently transferring these ions to the trap. In the near-trap geometry, the MALDI samples were positioned near the internal surface of the ring electrode (radial introduction) [10–12] or at one of the end cap electrodes (axial introduction) [13]. The generation of ions in an external ion source has obvious advantages, such as flexibility in the nature and size of the samples and switching of ion sources [14–17]. Despite the attractiveness of a MALDI-ITMS instrument outlined above, these investigations encountered several problems revealing that this coupling is not trivial. Crucial among these is the efficiency in the trapping of the MALDI ions. Ions produced by MALDI have wide, mass-independent velocity distributions [18]. Therefore, difficulties in the trapping of ions over wide mass ranges without large (mass-dependent) losses can be expected. In the early experiments, no sophisticated trapping schemes were employed, and the MALDI ions are injected into a constant trapping field (static trapping). Trapping is realized by reducing the kinetic energy of the ions to a value lower than the trapping potential set by the rf field by means of collisions with buffer gas molecules. Several theoretical studies have discussed this process [19–21] and experiments utilizing this method of trapping have been reviewed extensively [22,23]. The main drawback of this method is found to be a mass-dependent, relatively low, trapping efficiency, where the amplitude of the rf field is found to determine the ion mass at which maximum trapping efficiency occurs [24,25]. Several new methods have been developed to improve the trapping of ions produced in a pulsed ionization technique. It has been demonstrated that the ion potential energy can be reduced if the rf field is switched on after the ions reached the central region of the trap, whereas it is gated off during ion injection [26]. Following an alternative method, which is called dynamic trapping [27–29], the rf field is initially set to a low level to allow the ions an easy penetration of the trapping field. Subsequently, the amplitude of the trapping field is rapidly ramped to a high level to realize trapping before the ions have reached the opposite trap boundary and are lost. In the case of a near-trap geometry, dynamic trapping was demonstrated to give an improvement in the trapping efficiency of one order of magnitude [13]. In a more subtle version, called matched dynamic trapping [30], the trapping efficiency was found to be improved by an additional factor of 4 for an external source geometry. This improvement was accomplished by initially ramping the amplitude of the trapping field to even a higher level, followed by a down ramp to a lower level. Finally, it was demonstrated that also applying a dc retarding voltage to the end-cap electrodes improves trapping efficiency [21].

The second essential problem encountered in MALDI-ITMS experiments results from the strong dependence of the performance of the ion trap mass

spectrometer on the total number of ions that are stored inside the trap. When the ion population within the ion trap becomes too dense, then the electrical fields to which the ions are being subjected are substantially modified by the electrostatic forces associated with the trapped ions, that is, the space-charge. Low levels of space-charge result into slight shifts in the secular frequencies of the ions [31–33], which are observed as small shifts in the mass assignment. At higher space-charge levels, also peak broadening is observed, up to levels at which the analyzer performance is seriously degraded [34]. These space-charge effects are especially in the case of MALDI measurements easily encountered, because the MALDI process will generate a large excess of matrix ions in addition to the ions of interest. The most straightforward method for diminishing the ion population inside the trap is optimizing the amplitude of the rf field to satisfy $q_z > 1$ for the matrix ions and $q_z < 1$ for the analyte ions, which means that only the polymer ions will be trapped. The disadvantage of this method is (next to the previously mentioned relatively low trapping efficiency) that this amplitude does not necessarily provide optimal trapping for the ions under study. Another option is ejection of the matrix ions from the trap during or after trapping [35]. In the case of dynamic trapping in an external source geometry matrix ion discrimination is also feasible on basis of differences in flight-times [17]. During the transport to the trap, the low-mass matrix ions separate in space from the higher mass analyte ions and therefore these will arrive earlier at the trap entrance. Appropriate adjustment of the timing in ramping the amplitude of the rf trapping field should accomplish the desired discrimination.

In this paper, we describe the design and performance of a new external ion source MALDI-ITMS instrument. No sophisticated trapping schemes were employed in the presented experiments during ion injection into the ion trap. The performance of the instrument, in particular with respect to mass dependencies in trapping efficiency and mass shifts due to space-charge effects, was investigated by measuring the molecular weight distributions of low-molecular weight synthetic polymer samples. These samples are ideal for this purpose for two reasons. The first reason is that the polymer distributions cover substantial mass ranges and mass dependencies in the trapping efficiency will therefore be reflected in distortions of the measured distributions. These distortions were quantified by comparing the MALDI-ITMS distributions with the distributions measured by MALDI-TOF and previously published results obtained by MALDI-FTICR-MS. On basis of these results it was possible to determine the optimal experimental conditions for measuring the molecular weight distribution of a complex block copolymer sample without significant distortions. Evaluation of the distributions in the individual block lengths demonstrated that mass discrimination effects were negligible in the copolymer measurements. The second reason is that this type of samples is demanding for the total number of trapped ions. Polymer distributions generally consist of many components. This means that the total ion signal is divided over the different components and therefore it is necessary to accumulate many ions in order to obtain an adequate signal-to-noise ratio for each component. Consequently, mass shifts induced by the total associated space-charge are likely. These mass shifts were monitored in detail as a function of the total ion load on basis of deviations in the mass difference between adjacent components in a single spectrum. In the final series of measurements on a complex polymer sample it is demonstrated that carefully controlling the total space-charge in the trap sufficiently minimizes these shifts. This is illustrated on basis of end group mass determinations with an accuracy of ∼0.1 u from the measured spectra.

2. Experimental

2.1. MALDI-ITMS

Fig. 1 shows a schematic representation of the newly constructed MALDI-ITMS instrument. In this instrument, the ions are generated external to the ion trap in a home-build MALDI ion source, which is identical

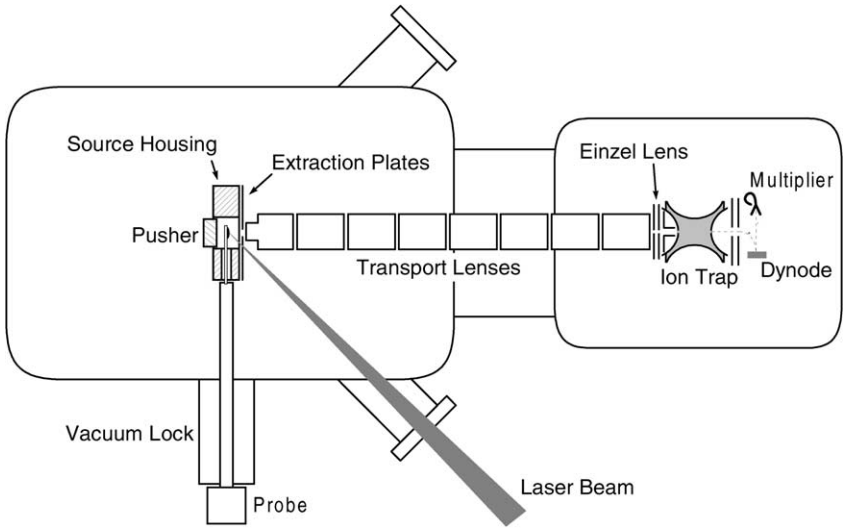

Fig. 1. Schematic overview of the instrument for MALDI-ITMS experiments.

to the one in our MALDI-FTICR-MS instrument [36]. These are subsequently accelerated towards and focused onto the entrance of the ion trap using electrostatic ion optics. This ion trap (including the control electronics) was obtained from Bruker-Franzen Analytik GmbH (Bremen, Germany), and is identical to the one in the commercial Bruker Esquire instrument.

The MALDI samples were deposited on the stainless steel tip of a direct insertion probe. This probe was inserted into the external ion source via a vacuum lock. After insertion, it was in electrical contact with the source housing. The frequency-tripled output of a Quanta-Ray GCR-11 (Spectra-Physics Inc., Mt. View, California) pulsed Nd:YAG laser (producing 355 nm pulses with an energy of 60 mJ and a pulse length of 5 ns) was focused onto the MALDI probe with an incident angle of 45°. The area at the MALDI probe illuminated by the laser beam was approximately 2 mm × 1 mm and the power density on target was measured to be maximally 100 MW/cm^2. The ions were created at a potential of typically 15 V and extracted from the ionization region by applying a potential difference of approximately 10 V between the source housing and the extraction plates. Subsequently, they are alternately accelerated and decelerated between 80 and 30 eV in a modified Heddle geometry, consisting of eight elements, to transport the ions over the distance of 0.2 m between the MALDI source and the ion trap. At the end of the transport lenses a set of three electrodes, operated at −40, −150, and −10 V, was installed to focus the ion beam onto the entrance of the ion trap. The ions are injected into the active trapping field of the ion trap, and He background gas was introduced into the ion trap at an estimated pressure of 10^{-3} mbar to realize trapping by collisional cooling of the ion kinetic energies.

At the beginning of each experiment the laser was triggered by a TTL pulse from the ion trap control electronics. A delay of typically 70 ms was employed allowing the ions to travel from the source to the cell, and to translationally cool to the center of the trap. The amplitude of the rf voltage during ion injection was determined by the value of the so-called cut-off mass $M_{\text{cut-off}}$, which corresponds to the mass of the ions that are in resonance with the dipole field at that amplitude. The relation between the amplitude and the cut-off mass is in the standard operation mode given by

$$V_{\text{rf}} = \frac{8.2}{e}\Omega^2 r_0^2 M_{\text{cut-off}}$$

Table 1
The four modes of measuring and the corresponding operational parameters that are available in the Bruker software

Mode of measuring	Mass range	Scan speed (u/s)	Maximum scan width[a]	Frequency resonant ejection voltage
Standard	50–2000	∼2000	800	$\Omega/3$
Standard–high resolution	50–2000	∼1000	400	$\Omega/3$
Extended	50–3400	∼3400	1200	$\Omega/6$
High	100–6000[b]	∼3400	1200	$\Omega/11$

[a] Maximum scan width for which it is possible to store the complete multiplier signal as function of time.
[b] The upper mass limit for the high mass mode was restricted due to software limitations during the measurements presented in this paper to 3400 u.

Here, V_{rf}, e, Ω, and r_0 are the amplitude of the rf field, the elementary charge, the frequency of the rf field, and the radius of the trap (10 mm), respectively. Finally, the mass spectrum was recorded in the resonant ejection technique by scanning the amplitude of the rf voltage on the ring electrode and the phase-locked resonant ejection voltage over the two end caps. The frequency of the rf voltage was 781 kHz and its maximum amplitude was 20 kV_{pp}. The scan rate of the rf voltage and the frequency of the resonant ejection voltage are listed in Table 1 for the different modes of measuring. Ejected ions were accelerated over 7 kV towards a conversion dynode and the secondary electron signal was recorded by a channeltron detector operated at −1.2 kV. The entire multiplier signal as function of time was stored if only limited mass ranges were examined (where the maximum width of the mass range depends on the mode of measuring and is included in Table 1). Otherwise, the multiplier signal was converted in a bar. In that case the signal intensity is only stored for integer masses. The software packages Bruker DataAnalysis and m.a.c.s Labstar (Bruker-Franzen Analytik GmbH, Bremen, Germany) running on an IBM compatible computer under OS2 controlled the measurements and performed data acquisition and processing.

2.2. MALDI-TOF-MS

Reference spectra of the samples used to characterize the performance of the MALDI-ITMS instrument were recorded by MALDI-TOF-MS. In this instrument, a Bruker Reflex mass spectrometer, desorption and ionization is achieved using a nitrogen laser, which produces 337 nm pulses with a pulse length of 5 ns. Samples for the MALDI experiments were deposited on a stainless steel disk containing 26 targets. After drying, this disk was transferred into the mass spectrometer via a vacuum lock. A CCD camera, connected to a video monitor, allowed visual selection and examination of the area of laser interaction with the sample. Selection of the MALDI target and positioning of the target under the desorbing laser beam were computer controlled. Optimization of the MALDI signal was achieved by varying the laser power and the position of the desorption spot. The spot size on the sample surface was approximately 50 μm in diameter. The laser beam was attenuated using a variable neutral density filter. The laser irradiance was typically optimized to be slightly above threshold. During measurements, a source pressure of $\sim 10^{-6}$ mbar and analyzer pressure of $\sim 10^{-7}$ mbar was maintained. Ions were detected in the linear mode using an accelerating voltage of 20 kV and a detector voltage of 1000 V by a MCP detector (1 GHz A/D converter). All spectra were signal averaged over 100 laser shots. All time of flight spectra were calibrated using a mixture of PEG1000, PEG2000 and PEG3000.

2.3. Sample preparation

The poly(methyl methacrylate) (PMMA) standards were obtained from Polymer Laboratories (Amherst, MA). Four different standards were studied with an average molecular weight of 640, 1140, 1850, and 3100 u, respectively. With these standards, also a

polymer blend with an extremely large polydispersity was obtained by mixing these in ratio to their number-averaged molecular weight. The polyethylene glycol (PEG) sample with average molecular weight of 1000 u was obtained from Serva (Heidelberg, Germany). Also the Jeffamine D2000 is commercially available (Texaco Chemical Company). According to the manufacturers data sheet (SC-024 102-0411), the Jeffamine D2000 is an amine-terminated polypropylene glycol with the general structure $H_2N–(C_3H_6O)_n–C_3H_6NH_2$. The PLURONIC L31 is a tri-block copolymer of poly(ethylene oxide) poly(propylene oxide) and was obtained from BASF (Mount Olive, NJ). The average molecular weight of the propylene oxide part was specified to be 950, and the ethylene oxide fraction of the final polymer sample was specified to be 20%. Liquitex acrylic phtalocyanine blue paint was manufactured by Lefranc & Bourgeois (Le Mans, France). The matrix in the MALDI experiments was 2,5-dihydroxybenzoic acid (DHB) from Sigma Chemical Co. (St. Louis, MO).

The polymer samples were prepared for MALDI mass spectrometry by mixing a 1-M matrix solution in ethanol with an approximately 10-g/L analyte solution in ethanol yielding a molar ratio matrix:analyte = 1000:1. For the experiments on PMMA the analyte solutions were first mixed yielding unity molar ratios. The resulting mixture was electrosprayed onto a stainless steel probe tip [37]. Approximately 0.1 mL analyte/matrix is consumed during sample deposition. The acrylic paint was applied to the probe without prior sample preparation (i.e., direct laser desorption instead of MALDI was performed). The total sample loading on the probe was approximately 10 ng. Each sample was used to produce ions for thousands of laser shots by rotating the sample probe over 360° and translating it over ∼5 mm (in this way a total area of ∼30 mm^2 could be exposed to the laser spot).

3. Results

3.1. Evaluation of mass dependencies in the trapping efficiency with broad polymer distributions

Characterization of the blend of PMMA standards was realized by measuring a MALDI-TOF-MS reference spectrum. This spectrum was obtained by averaging 100 laser shots and is shown in Fig. 2. It demonstrates that the molecular weight distribution

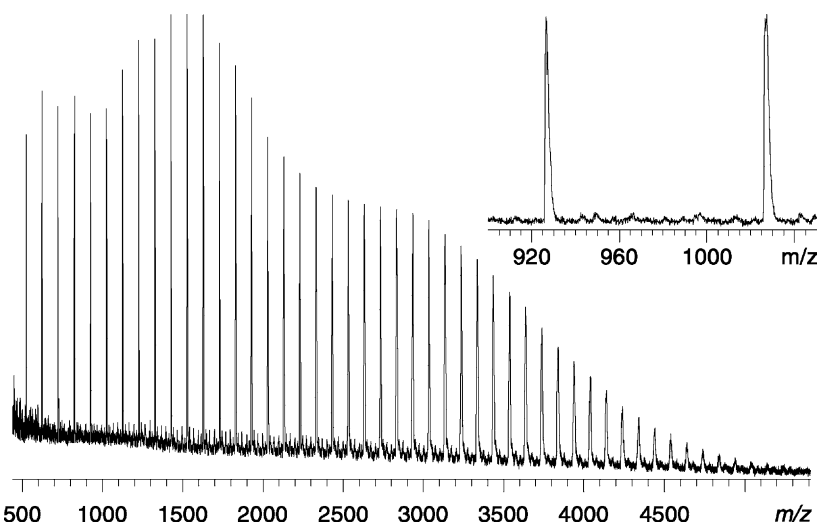

Fig. 2. Reference spectrum of the PMMA blend recorded by MALDI-TOF. The expansion of the mass scale show that primarily sodium cationized species are observed and that the resolution is insufficient to resolve the isotopic patterns.

of the PMMA blend ranges from m/z 500 (corresponding to a degree of polymerization $n = 5$) to 5500 ($n = 55$). The expansion of the mass scale illustrates that predominantly sodium cationized pseudo-molecular ions are formed in the MALDI process. It further reveals that the resolution in the MALDI-TOF experiment is insufficient to distinguish between the natural occurring $^{12}C/^{13}C$ isotopes. No further optimization of the resolution was attempted because only information on the shape of the molecular weight distribution was required. The MALDI-TOF molecular weight distribution is characterized by calculating the molecular weight averages from the spectrum in Fig. 2. For these calculations, the measured masses were corrected for the mass of the sodium adducts and the intensities were determined by integration over the complete isotopic patterns. The calculated averages are the number-average molecular weight ($M_n = \Sigma(N_i M_i)/\Sigma N_i$, where N_i and M_i denote the signal intensity and measured mass at peak i), the weight-average molecular weight ($M_w = \Sigma(N_i M_i^2)/\Sigma(N_i M_i)$), the z-average molecular weight ($M_z = \Sigma(N_i M_i^3)/\Sigma(N_i M_i^2)$), and the polydispersity index (M_w/M_n). The results are listed in Table 2. It is assumed that the ion distribution generated in the ion source of our MALDI-TOF-MS is identical to the distribution generated in the external ion source of our MALDI-ITMS.

Next, the same sample was analyzed in the MALDI-ITMS instrument to monitor mass dependencies in the trapping efficiency of the instrument. The mass range m/z 500–3400 was examined in the high-mass mode (as was mentioned before, m/z 3400 is presently the software imposed upper mass limit of the system). In a series of experiments, the amplitude of the active rf field (that is, the value of $M_{\text{cut-off}}$) was varied because this parameter was expected to primary determine the relationship between trapping efficiency and ion mass [24,25]. In each experiment, spectra were recorded during 80 successive laser shots. The resulting total ion current (TIC, the overall intensity in the individual scans as a function of time) for the experiment with $M_{\text{cut-off}} = 100$ u is presented in the upper plot in Fig. 3. This plot shows that the MALDI-ITMS experiments are subjected to large shot-to-shot variations. The origin of these shot-to-shot variations is not likely to be in the MALDI ion source for two reasons. First, the ionizing laser beam has been tested to be stable in the course of the measurements, and second, MALDI experiments on our MALDI-FTICR-MS instrument utilizing an identical MALDI ion source did not reveal such large variations. Also the instabilities in the ion transport are not expected to be the cause, because previous experiments utilizing continuous ion beams did not reveal large temporal variations in the total ion yield. Therefore, we presently attribute the observed shot-to-shot variations to changes in the trapping efficiency due to random variations in the phase of the rf trapping field at the laser firing [29]. Elimination of the shot-to-shot variations was achieved by averaging the individual scans composing the TIC-signal, yielding the top spectrum of Fig. 3. The other spectra in Fig. 3 were similarly obtained with $M_{\text{cut-off}} = 150$, 200, 250, and 300 u, respectively. Experiments performed with $M_{\text{cut-off}}$ smaller than 100 u or larger than 300 u were observed to give no significant signals. It is immediately seen from this set of spectra that the shape of the measured molecular weight distribution, and thus the mass range of efficient trapping, is strongly dependent on the setting for $M_{\text{cut-off}}$. The resulting distortions in the observed molecular weight distributions are nicely reflected by the characterizing weight averages. These have been calculated for the individual spectra in Fig. 3 and are included in Table 2. As expected from the measured spectra, the weight averages

Table 2
The characterizing weight averages of the PMMA blend, determined from the TOF measurement in Fig. 2 (column 2) and from the IT measurements in Fig. 3 for different cut-off settings (columns 3–7)

	TOF	ITMS (u)				
		100	150	200	250	300
M_n	2094	1363	1668	2106	2348	2466
M_w	2644	1544	1810	2265	2486	2586
M_z	3085	1720	1955	2408	2604	2688
M_w/M_n	1.26	1.13	1.09	1.08	1.06	1.05

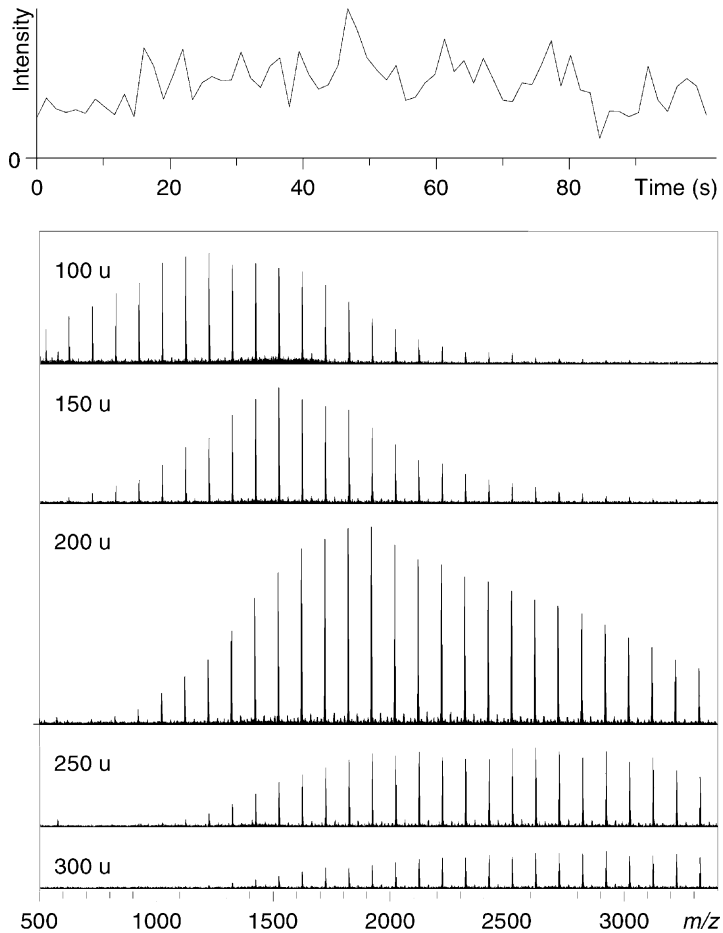

Fig. 3. MALDI-ITMS measurements of the poly(methyl metacrylate) blend. The five spectra are recorded for the different values of $M_{\text{cut-off}}$ indicated in the spectra. The total ion current is plotted as a function of time in the upper plot during the 80 laser shots which comprise the spectrum for $M_{\text{cut-off}} = 100$ u.

increase for increasing $M_{\text{cut-off}}$. In a rough approach, the number-average molecular weights are indicative for the center of the mass range in which optimal trapping occurs at a given setting of $M_{\text{cut-off}}$. Unfortunately, the exact relationship between the trapping efficiency (as a function of mass) and $M_{\text{cut-off}}$ cannot be obtained. This is caused by the mass discrimination effects due to space-charge, which cannot be recovered from the present measurements. The observed decrease of the polydispersity index for increasing $M_{\text{cut-off}}$ is mainly the result of the upper mass limit of m/z 3400 in the MALDI-ITMS experiments. After all, the spectra in Fig. 3 suggest that for $M_{\text{cut-off}} \geq 200$ u components with m/z >3400 would be detected if the upper limit could be extended to m/z 5000, which would lead to higher values of the polydispersity factor.

3.2. Characterization of the trapping efficiency

It follows from the previous experiments that, in order to characterize the trapping efficiency as a function of mass for different amplitudes of the active rf field, it is necessary to minimize mass discrimination effects due to space-charge. This was accomplished by evaluating the PMMA standard with an average molecular

weight of 640 u for different values of $M_{cut\text{-}off}$ and comparing the results with a MALDI-TOF-MS reference spectrum. The PMMA640 sample has a much more moderate polydispersity index in comparison to the PMMA blend, which means that the number of trapped ions can be controlled to be much lower. The MALDI-TOF-MS reference spectrum is plotted in Fig. 4A and shows the entire distribution, ranging from m/z 425 to 1525 ($n = 4$–15) and with its maximum at m/z 725. The MALDI-ITMS experiments were performed in the standard mass range for $M_{cut\text{-}off}$ ranging from 50 to 180 u in steps of 10 u. The individual spectra were averaged over 25 laser shots. As an example, the MALDI-ITMS spectrum recorded with $M_{cut\text{-}off} = 60$ u is shown in Fig. 4B. This reveals again a severe distortion in the mass distribution recorded by the MALDI-ITMS instrument. The trapping efficiency was determined as a function

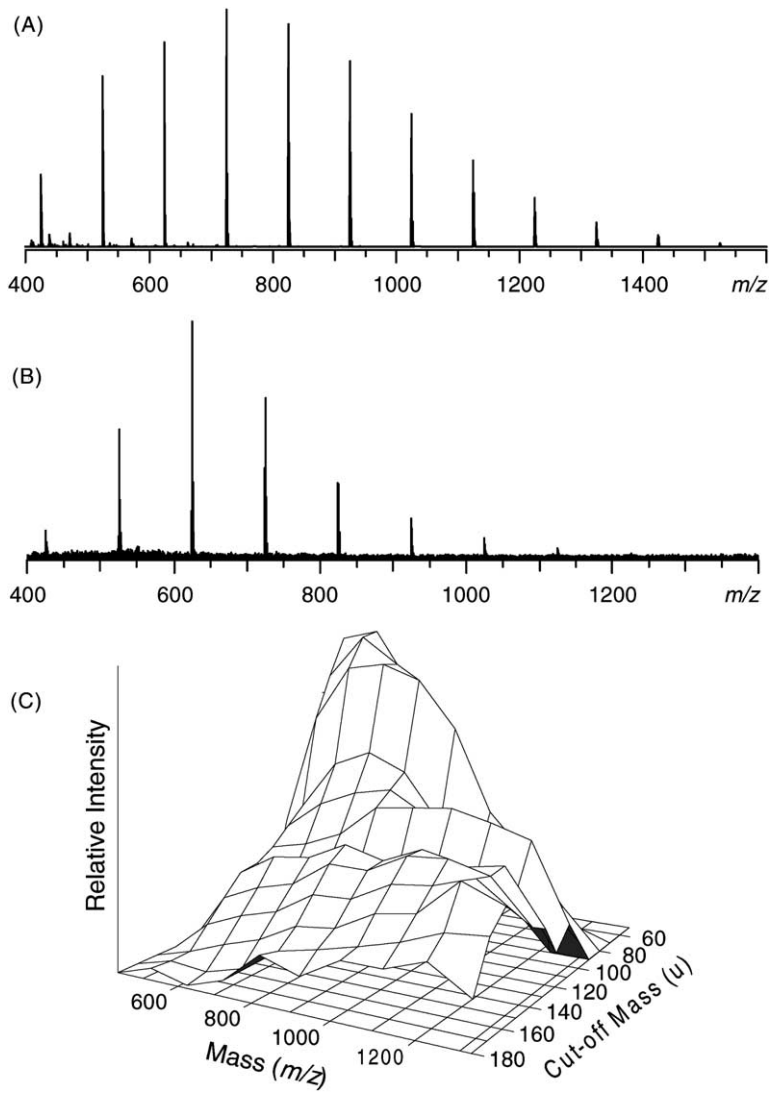

Fig. 4. Molecular weight distribution of PMMA640 recorded by MALDI-TOF (A); by MALDI-ITMS with $M_{cut\text{-}off} = 60$ u (B); and by MALDI-ITMS as a function of the value of $M_{cut\text{-}off}$ (C).

of mass and $M_{\text{cut-off}}$ by dividing the relative intensities in the series of MALDI-ITMS spectra by those in the MALDI-TOFMS spectrum:

$$P(M_i, M_{\text{cut-off}}) = \frac{I_i^{\text{ITMS}}}{I_i^{\text{TOF}}}$$

Here, I_i^{ITMS} and I_i^{TOF} are the intensity of the polymer component measured by MALDI-ITMS and the intensity of the same polymer component measured by MALDI-TOF, respectively, at mass M_i, and P is the trapping efficiency. The results are visualized as a function of $M_{\text{cut-off}}$ in the 3D plot in Fig. 4C. The 3D plot suggests that for $M_{\text{cut-off}} > 90$ u the trapping efficiency becomes fairly constant over considerable mass ranges. For example, at $M_{\text{cut-off}} = 120$ u the PMMA distribution measured by MALDI-ITMS was almost identical to the one measured by MALDI-TOF-MS in the mass range m/z 600–1200.

This "flatness" of the detection efficiency curve was examined in more detail by evaluating the distributions in the individual components of the PLURONIC L31 block copolymer. This sample was previously characterized with MALDI-FTICR-MS [38], and there it was found to follow the so-called random coupling hypothesis, that is, there exists no correlation between the lengths of the different constituents. A correlation between these lengths in the final results will therefore be indicative for mass discrimination effects which distort the measured molecular weight distribution.

The PLURONIC copolymers are fabricated by first synthesizing a poly(propylene oxide) polymer and subsequently adding ethylene oxide units to both sides of the initial poly(propylene oxide) polymers which yields a distribution of tri-block polymers of the type HO–$(C_2H_4O)_m$–$(C_3H_6O)_n$–$(C_2H_4O)_0$–H. Fig. 5 shows the MALDI-ITMS spectrum. In order to obtain

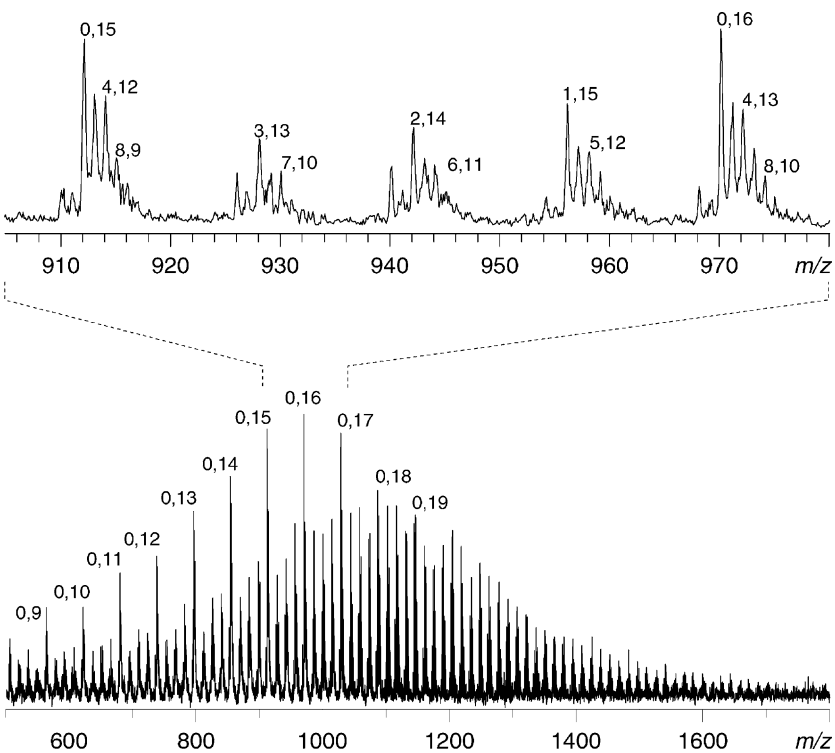

Fig. 5. MALDI-ITMS spectrum of PLURONIC L31. For this measurement $M_{\text{cut-off}}$ was optimized to minimize mass discrimination over the mass range covered by the molecular weight distribution. The series of poly(propylene glycol) homopolymers is indicated (the first number refers to n^{EO}, the second number to n^{PO}). In the expanded mass scale the composition of all monoisotopic copolymers is indicated.

this spectrum, two experiments were performed over the mass ranges *m*/*z* 500–1300 and *m*/*z* 1100–1900, respectively, in which 50 laser shots were averaged in the standard mass mode with $M_{\text{cut-off}} = 70$ u. In this way it was possible to store the complete multiplier signal as function of time and thus to preserve peak information. The overall spectrum was reconstructed by overlaying the two individual spectra. The mass range shown covers the entire molecular weight distribution. Spiking the samples with sodium, potassium, and lithium salts verified that only sodium adduct ions are present in the spectrum. The most dominant ion series was identified as the distribution of the poly(propylene oxide) homopolymers. The composition of the copolymer molecules is indicated for the series of poly(propylene glycol) homopolymers in the spectrum, and in the expanded mass scale for all monoisotopic peaks. Here the first number refers to the number of ethylene oxide units present in the copolymer (n^{EO}) and the second number refers to the number of propylene oxide units present (n^{PO}). In this way, we have identified all the components with S/N > 2, yielding 210 peak intensities and corresponding copolymer compositions.

Before evaluating the individual block length distributions two effects have to be considered. Firstly, it can be seen from the expanded mass scale that no distinction can be made between the second isotopic peak of the homopolymer with $n^{\text{EO}} = 0$ and $n^{\text{PO}} = 16$ (monoisotopic peak at *m*/*z* 969.6) and the monoisotopic peak of the copolymer with $n^{\text{EO}} = 4$ and $n^{\text{PO}} = 13$ at *m*/*z* 971.6. Secondly, it is evident that taking the intensity of monoisotopic peaks to be representative for the relative abundance of the corresponding component will introduce errors as the relative abundance of the monoisotopic peak will significantly vary over the mass range under study. A previous publication has dealt with these problems and proposed a correction method to reveal the actual relative abundance's [38]. After applying this correction method to the data obtained from Fig. 5, the corrected peak intensities are plotted as a function of n^{EO} and n^{PO} in Fig. 6. The contour plot reveals that the distribution in the propylene oxide block remains approximately constant for the different total lengths of the ethylene oxide blocks. This result demonstrates that our MALDI-ITMS instrument can be optimized to have a constant trapping efficiency in the mass range *m*/*z* 500–1500. On basis of the results presented above, it is expected that this applies to any mass interval below *m*/*z* 3400 and a width less than ~1000 u.

3.3. Mass shifts induced by space-charge

The dependence of the measured mass upon the signal intensity has been investigated for a phtalocyanine

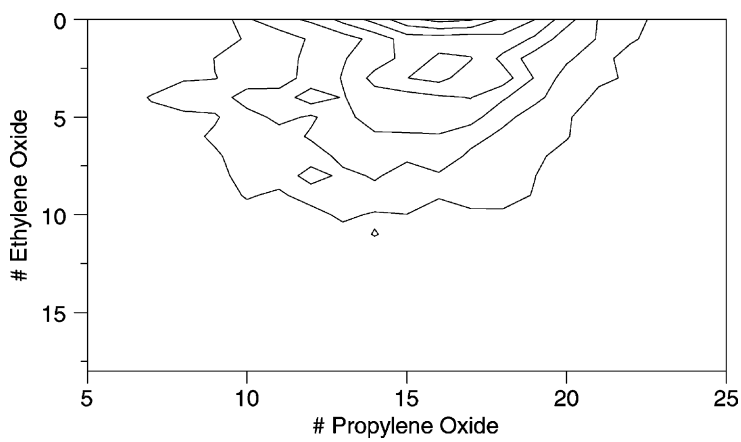

Fig. 6. Contour map of the distribution of monomer units as a function of the individual monomer units in the polymer. The data plotted are extracted from the spectrum in Fig. 5.

blue pigment in a series of measurements on the acrylic paint sample. For these experiments the complex paint formulation was applied directly to the probe, i.e., direct laser desorption was employed instead of MALDI. Spectra were recorded for single laser shots in the high-resolution mode with $M_{\text{cut-off}} = 100$ u over the mass range m/z 400–700. Variations in the intensity of the molecular ion were induced by changes in the attenuation of the laser beam at the one hand, and by the statistical shot-to-shot variations in the MALDI-ITMS experiments at the other hand. The intensity of the molecular ion cluster was determined by integration of the ion signal over the mass range m/z 574–560. The monoisotopic peak of the molecular ion cluster was fitted with the Gauss function $I_{\text{meas}} = A\exp(-(m_{\text{meas}} - m_{\text{c}})^2/w^2)$, where I_{meas} was the measured intensity at mass M_{meas}. The fit result for the peak center M_{c} was taken as the measured mass of the pigment. The fit results for the peak height (A) and the peak width (w) were not evaluated. The results are plotted in Fig. 7. The plot indicates that a linear relationship exists between the measured mass and the molecular ion intensity for intensities lower than 4×10^6 cps. The increase in the measured mass for an increasing ion load can be explained by realizing that the mass axis (y-axis) can be regarded as a time-of-ejection axis, whereas the intensity of the molecular ion (x-axis) can be regarded as the total number of ions present inside the trap. It is evident that the space-charge associated to the ion cloud inside the trap slightly shields the electrical field induced by the rf voltage on the ring electrode. This shielding increases for increasing numbers of ions, inducing a decrease of the effective electrical field strength. As a result of the decreased effective electrical field, the secular motion of ions with a particular m/z will get in resonance with the alternating dipole field across the end caps at higher rf voltages, and thus will be ejected and detected at later times (i.e., at higher masses). The asymptotic behavior of the plot for intensities larger than 4×10^6 cps is presently not fully understood.

The inset in Fig. 7 shows the measured isotopic pattern for an integrated intensity of 0.5×10^6 cps (upper spectrum) and 7×10^6 cps (lower spectrum), respectively, revealing the total mass shift of ~1.1 u over the complete set of measurements. It further shows that

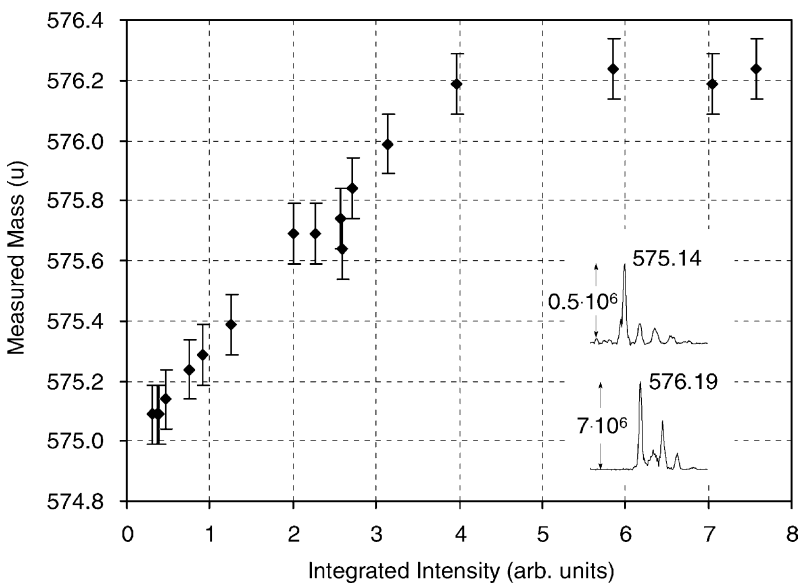

Fig. 7. Mass of the phtalocyanine blue pigment measured by LD-ITMS as a function of the intensity of the molecular ion (determined by integration over the entire isotopic pattern).

the isotopic pattern (both with respect to intensity as to spacing) are distorted at higher intensities. Inspection of the individual spectra revealed that the isotopic pattern becomes distorted for intensities larger than $\sim 1.5 \times 10^6$ cps. This suggests that it is possible to keep the mass variations within reasonable limits (in this case within a range of approximately 0.3 u) by optimization of the total ion current on basis of the shape of the isotopic patterns.

After the previous results, which only concerned ions of one specific mass, it is interesting to investigate shifts in the measured mass of a particular ion induced by the presence of ions at other masses. This was studied by measuring the distribution of the poly(ethylene glycol) sample. Mass spectra were produced by averaging 25 spectra from individual scans in the extended mass range with $M_{\text{cut-off}} = 90$ u, covering the molecular weight distribution in the mass range m/z 745–1362 (corresponding to a degree of polymerization of 16 and 30, respectively). First, the distribution was measured with the laser intensity just above threshold, which implies that mass shifts are minimal. The instrument was calibrated on basis of this measured distribution. Next, a spectrum was taken at a much higher laser intensity. The influence of the total ion load on the measured mass was evaluated by plotting the difference between the mass determined from the spectrum and the calculated mass as a function of the number of ions trapped at the time of ejection for each monoisotopic peak in the spectrum. The latter quantity was assumed to be proportional to the integration of the ion signal starting two mass units lower than the mass of the ejected ions up to the upper limit of the mass scan. The result is plotted in Fig. 8. The corresponding high-intensity MALDI-ITMS spectrum is shown in the inset in Fig. 8. It should be noted that $M_{\text{cut-off}}$ was optimized for optimal signal-to-noise and no attempt was made to produce a molecular weight distribution close to the expected one. The linear dependence between the mass shift and the integrated intensity demonstrates that shifts in the measurement of an ions mass are entirely determined by the magnitude of the total space-charge

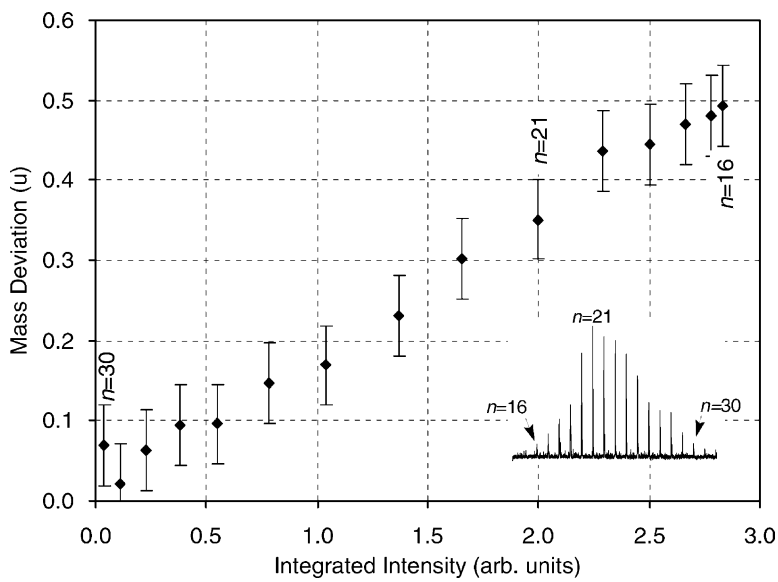

Fig. 8. Mass deviations as a function of the integrated intensity for a PEG1000 sample measured by MALDI-ITMS. The mass deviation is defined as the difference between the measured mass of a particular component of the molecular weight distribution and its actual mass. The corresponding integrated intensity is determined by integration of the mass spectrum over the mass range starting at (and including) this particular component up to the upper limit of the measured mass range. This quantity is assumed to be proportional to the magnitude of the trapped ion population at the time of its ejection.

at the time of ejection. An important consequence of this result is that the number of trapped ions does not change the calibration function by a constant offset. Instead, the change depends on both the masses as well as the intensities of all trapped ions, and a complex calibration function which is hard to predict is the result.

It is obvious that mass shifts can be very significant in the identification of elemental compositions from exact mass measurements. A challenging test for the possibilities of MALDI-ITMS with respect to accurate mass measurements is therefore the determination of the polymer end groups in a complex polypropylene sample. According to the specifications of the manufacturer the Jeffamine D2000 sample consists of a distribution of amine terminated polypropylene glycols with the general structure $[H_2N–(C_3H_6O)_n–C_3H_8N + Na]^+$, having an average molecular weight of 2000 u. As was mentioned before, the present set-up only allows to acquire scan spectra in standard mass mode over mass ranges smaller than 800 u. In order to preserve information on single isotopic peaks, experiments were performed in the standard mass mode with $M_{\text{cut-off}} = 70$ u over three different mass ranges, namely *m*/*z* 500–1300, *m*/*z* 1100–1900, and *m*/*z* 1700–2500, respectively. In this way the complete molecular weight distribution of the Jeffamine sample was covered. The laser intensity was optimized to be just above threshold. Spectra of 50 individual scans were summed for each of the three mass ranges. First, these settings were used to record spectra of the PMMA1140 standard (data not shown) for calibration the instrument. The results of the experiments on the Jeffamine sample are combined in Fig. 9 to reconstruct the complete molecular weight distribution. It is seen that the molecular weight distribution covering the mass range *m*/*z* 500–2500 is bimodal, pointing to contamination with other polymers, early termination reactions during polymerization, or oxidation. The expansion of the mass scale reveals that the resolution $(m/\Delta m)_{50\%}$ of 2500 at *m*/*z* 1722 is sufficient to resolve the naturally occurring $^{12}C/^{13}C$ isotopes of the component molecules. Only sodium adduct ions are present in the spectrum, as was again verified by spiking the samples with sodium and potassium salts. The distribution was characterized by calculating the molecular weight averages and the polydispersity index from the intensities of all monoisotopic peaks in the spectrum. The results are listed in Table 3. Also the results of previous analysis on the same sample by MALDI-FTICR-MS [39] are included. It is seen that the average molecular weights obtained from the ITMS data are structurally lower than those obtained from the FTICR-MS data. This results from an optimization of the value for $M_{\text{cut-off}}$

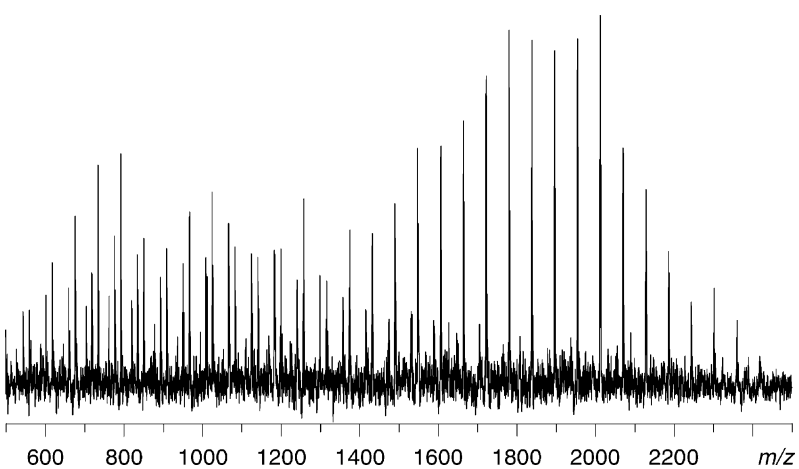

Fig. 9. MALDI-ITMS spectrum of Jeffamine D2000. The value of $M_{\text{cut-off}}$ was optimized for optimal signal-to-noise at the lower mass end of the molecular weight distribution.

Table 3
M_n, M_w, M_z, and M_w/M_n values calculated from the molecular weight distributions of Jeffamine D2000 measured by MALDI-FTICR-MS [39] and MALDI-ITMS (Fig. 9)

	MALDI-FTICR-MS	MALDI-ITMS			
	Complete MWD	Complete MWD	C_3H_8N	C_3H_5	C_3H_5O
M_n	1559	1347	1785	997	912
M_w	1746	1517	1817	1062	958
M_z	1779	1653	1847	1119	1002
M_p	1779	1779	1779	1067	793
M_w/M_n	1.12	1.13	1.02	1.07	1.05

for especially the lower mass range (there signal intensities are lower). Consequently, masses above m/z ~1600 were slightly discriminated which causes the average molecular weights to be underestimated.

End group analysis [37] of the mass spectrum of the Jeffamine D2000 spectrum yielded that there are at least three different series of peaks at equidistant intervals of 58 u present in the molecular weight distribution of Jeffamine D2000. The masses of the end groups $M_{end,meas}$ were calculated by subtracting the mass of the cationizing species and the product of the degree of polymerization and the mass of the repeating unit from the measured masses for each component in the molecular weight distribution. Subsequently, these values were averaged for the three series of peaks. The results are presented in Table 4, along with a proposal for the elemental composition of the end groups, the corresponding calculated masses of the end groups $M_{end,calc}$, and the differences between the measured and calculated end group masses ΔM_{end}. In addition the characterizing molecular weights were calculated for the individual series, which are included in Table 3.

The results in Table 4 show that the dominant distribution in Fig. 9 consists of the amine terminated polypropylene glycols of the type $[H_2N–(C_3H_6O)_n–C_3H_8N + Na]^+$, as specified by the manufacturer. The molecular weight distribution of this series ranges from m/z 1316 ($n = 21$) to m/z 2303 ($n = 38$) and exhibits a M_p of m/z 1779. The second prominent ion series is observed in the low molecular weight part of the spectrum, ranging from m/z 544 to 1473, and with a M_p of m/z 1067. End group analysis on this series yielded 57.26, which corresponds to the sum of the masses of C_3H_5 and NH_2 (Table 4). Such unsaturated structures are well known for poly-ethers, and may result from dehydration of terminal hydroxyl groups during polymerization. This would lead to early termination of the polymerization process, and thus explain the relatively low average molecular weight numbers of this series (Table 3). The last ion series is observed in the molecular weight range from m/z 560 to 1315 and exhibits a M_p of m/z 793. The mass of the corresponding end group was determined to be 73.25, which is in agreement with the sum of the masses of C_3H_5O and NH_2. This would indicate that for example oxidation processes have induced ketone or aldehyde functionalities in the polymer. In the MALDI-FTICR-MS experiments an additional ion series with an end group mass corresponding to the sum of the masses of H and NH_2 was observed. This ion series has not been recovered in the present investigation, as the resolution of the MALDI-ITMS experiment is not sufficient to resolve it from the naturally occurring ^{13}C isotopes of the $[H_2N–(C_3H_6O)_n–C_3H_5O + Na]^+$ series.

It can be concluded that the results of the end group analysis are in good agreement with those obtained from the previous MALDI-FTICR-MS experiments. This demonstrates that mass accuracies better than

Table 4
Masses and deviations in the end group analysis of Jeffamine D2000 by MALDI-ITMS

	$M_{end,calc}$	$M_{end,meas}$	ΔM_{end}
$H_2N–(C_3H_6O)_n–C_3H_8N$	74.08	73.96	−0.12
$H_2N–(C_3H_6O)_n–C_3H_5$	57.06	57.01	−0.05
$H_2N–(C_3H_6O)_n–C_3H_5O$	73.05	73.02	−0.03

0.3 u can be achieved by optimizing the laser intensity just above threshold.

4. Conclusions

The presented results clearly reveal that external ion source MALDI-ITMS experiments are easily complicated by mass discriminations and shifts in the mass determination. Mass discriminations are attributed to mass dependencies in the trapping efficiency because the amplitude of the rf field during injection highly determines the mass range of efficient trapping. Nevertheless, the instrument can be optimized to properly analyze samples with narrow mass distributions in a single experiment. This was demonstrated with the experimental confirmation of the random coupling hypothesis for the PLURONIC copolymer. On basis of the measurements of the PMMA blend it is expected that this generally holds for mass ranges smaller than ~1000 u up to at least *m*/*z* 3400. Analyses of systems that are more polydisperse are highly affected by mass discriminations. Possible experimental strategies for such samples are correction of the measured spectra for the mass discrimination or recording a series of spectra in which successive mass intervals of 1000 u are optimized for minimal mass discrimination. Of course, these remarks assume that additional mass discriminations due to space-charge can be avoided.

The shifts in the mass determination result from variations in the total space-charge. It was demonstrated that these can effectively be minimized by minimizing the number of trapped ions. At larger ion signals, mass shifts can be kept within reasonable limits if the shape of the isotopic patterns is evaluated. It was shown that these become substantially distorted when a mass shift of approximately 0.3 u is observed (see Fig. 7). This is however only true if the sample contains a few different components. Calibrant spectra have to be recorded to characterize the mass shifts for the actual experimental conditions if many different components are present in the ion population. This can be used to estimate the space-charge-induced mass shifts for the individual components on basis of shift versus ion intensity graphs (similar to Fig. 8) as a correction of the measured masses.

Acknowledgements

The authors gratefully acknowledge M. de Wilde and I. Stavenuiter for their technical assistance during the various stages of the experiment. Financial support for this work was provided by the foundation for Fundamenteel Onderzoek der Materie (FOM) and the Nederlandse Organisatie voor Wetenschappelijk Onderzoek (NWO, Dutch organization for scientific research). This work is part of Research Program 28 of FOM.

References

[1] F.B. Fenn, M. Mann, C.K. Meng, S.F. Wong, C.M. Whitehouse, Mass. Spectrom. Rev. 9 (1990) 37.
[2] F. Hillenkamp, M. Karas, R.C. Beavis, B.T. Chait, Anal. Chem. 63 (1991) 1193A.
[3] M. Karas, F. Hillenkamp, Anal. Chem. 60 (1988) 2299.
[4] M. Karas, U. Bahr, U. Giessmann, Mass Spectrom. Rev. 10 (1991) 335.
[5] M.V. Buchanan, R.L. Hettich, Anal. Chem. 65 (1993) 245A.
[6] Recent review, Anal. Chem.
[7] D.C. Schriemer, L. Li, Anal. Chem. 68 (1996) 2721.
[8] R.D. Edmondson, D.H. Russell, J. Am. Soc. Mass Spectrom. 7 (1996) 995.
[9] G.M. Alber, A.G. Marshall, N.C. Hill, L. Schweikhard, T. Ricca, Rev. Sci. Instrum. 64 (1993) 1845.
[10] D.N. Heller, I. Lys, R.J. Cotter, O.M. Uy, Anal. Chem. 61 (1989) 1083.
[11] V.M. Doroshenko, T.J. Cornish, R.J. Cotter, Rapid Commun. Mass Spectrom. 6 (1992) 753.
[12] D.M. Chambers, D.E. Goeringer, S.A. McLuckey, G.L. Glish, Anal. Chem. 65 (1993) 14.
[13] V.M. Doroshenko, R.J. Cotter, Rapid Commun. Mass Spectrom. 7 (1993) 822.
[14] K. Jonscher, G. Currie, A.L. McCormack, J.R. Yates III, Rapid Commun. Mass Spectrom. 7 (1993) 20.
[15] J.C. Schwartz, M.E. Bier, Rapid Commun. Mass Spectrom. 7 (1993) 27.
[16] A.W.T. Bristow, C.S. Creaser, Rapid Commun. Mass Spectrom. 9 (1995) 1465.
[17] J. Qin, J.M.M. Steenvoorden, B.T. Chait, Anal. Chem. 68 (1996) 1784.
[18] R.C. Beavis, B.T. Chait, Chem. Phys. Lett. 181 (1991) 479.
[19] R.K. Ghosh, A.S. Arora, L. Narayan, Int. J. Mass Spectrom. Ion Phys. 23 (1977) 237.

[20] C.-S. O, H.A. Schuessler, J. Appl. Phys. 52 (1981) 1157.
[21] C. Weil, M. Nappi, C.D. Cleven, H. Wolnik, R.G. Cooks, Rapid Commun. Mass Spectrom. 10 (1996) 742.
[22] R.E. March, R.J. Hughes, Quadrupole Storage Mass Spectrometry, Wiley, New York, 1989.
[23] J.F.J. Todd, Mass Spectrom. Rev. 10 (1991) 3.
[24] S.A. McLuckey, G.L. Glish, K.G. Asano, Anal. Chim. Acta 225 (1989) 25.
[25] K. Yoshinari, Y. Ose, Y. Kato, in: Proceedings of the 46th ASMS Conference on Mass Spectrometry and Allied Topics, Orlando, FL, 1998, p. 492.
[26] P. Kofel, in: R.E. March, J.F.J. Todd (Eds.), Practical Aspects of Ion Trap Mass Spectrometry, CRC Press, New York, 1995.
[27] G.C. Eiden, M.E. Cisper, M.L. Alexander, P.H.J. Hemberger, Am. Soc. Mass Spectrom. 4 (1993) 706.
[28] G.C. Eiden, A.W. Garrett, M.E. Cisper, N.S. Nogar, P.H. Hemberger, Int. J. Mass Spectrom. Ion Process. 136 (1994) 119.
[29] V.M. Doroshenko, R.J. Cotter, J. Mass Spectrom. 32 (1997) 602.
[30] J. Qin, B.T. Chait, Anal. Chem. 68 (1996) 2102.
[31] J.E. Fulford, D.N. Hoa, R.J. Hughes, R.E. March, R.F. Bonner, G.J. Wong, J. Vac. Sci. Technol. 17 (1980) 829.
[32] F. Vedel, M. Vedel, R.E. March, Int. J. Mass Spectrom. Ion Process. 99 (1990) 125.
[33] F. Vedel, M. Vedel, R.E. March, Int. J. Mass Spectrom. Ion Process. 108 (1991) R11.
[34] F.D. Williams, R.G. Cooks, Rapid Commun. Mass Spectrom. 7 (1993) 380.
[35] M.H. Soni, P.S.H. Wong, R.G. Cooks, Anal. Chem. 303 (1995) 149.
[36] R.M.A. Heeren, J.J. Boon, P. Caravatti, in: Proceedings of the 42nd ASMS Conference on Mass Spectrometry and Allied Topics, Chicago, 1994, p. 231.
[37] G.J. van Rooij, M.C. Duursma, R.M.A. Heeren, J.J. Boon, C.G. de Koster, J. Am. Soc. Mass Spectrom. 7 (1996) 449.
[38] G.J. van Rooij, M.C. Duursma, C.G. de Koster, R.M.A. Heeren, J.J. Boon, P.J.W. Schuyl, E.R.E. van der Hage, Anal. Chem. 70 (1998) 843.
[39] E.R.E. van der Hage, M.C. Duursma, R.M.A. Heeren, J.J. Boon, M.W.F. Nielen, A.J.M. Weber, C.G. de Koster, N.K. de Vries, Macromolecules 30 (1997) 4302.